

COMITATO NAZIONALE PER L'ENERGIA NUCLEARE
Laboratori Nazionali di Frascati

LNF-72/86
Ottobre 1972

G. Susinno : ANOMALOUS E. M. CURRENTS: EXPERIMENTAL.

Estratto da : Proceedings of the Informal Meeting on
Electromagnetic Interactions, Frascati, May, 1972.

ANOMALOUS ELECTROMAGNETIC CURRENTS (EXPERIMENTAL)

G. Susinno

Laboratori Nazionali del CNEN, Frascati

In these last years experimental results on the $\gamma n \rightarrow p\pi^-$ reaction have opened up some interesting theoretical questions.

From a comparison of the available data on the reaction $\gamma n \rightarrow p\pi^-$ with the inverse one ($\pi^- p \rightarrow \gamma n$) there seems to be some indication of a violation of time reversal invariance in electromagnetic interactions.

Furthermore, as has been discussed by G. Shaw in his talk, a comparison of π^+ and π^- photoproduction in the first resonance region seems to indicate the presence of an isotensor part in the hadronic e. m. current.

In the absence of an isotensor component the couplings of the γn and γp systems to the $A_{33}(1236)$ are equal. In particular one expects that the difference of the total cross section for π^- and π^+ production:

$$\Delta = \frac{k}{q} [\sigma_t(\pi^-) - \sigma_t(\pi^+)]$$

should be given by the slowly varying background only.

An eventual structure near the resonance in this difference would constitute evidence for an isotensor component in the $\gamma N A$ coupling. The existing experimental data have so far presented interesting but somewhat confusing features concerning this test.

In this talk I will discuss the present experimental situation regarding the $\gamma n \rightarrow p\pi^-$ reaction in view of the uncertainties surrounding it.

I refer to the talk by Shaw for discussion of the theoretical problems.

The information available comes from the following experiments :

- a) $\gamma n \rightarrow p\pi^-$: bubble chamber measurement by the ABHHM collaboration⁽¹⁾;
- b) $\gamma n \rightarrow p\pi^-$: bubble chamber measurement by the FNPR collaboration⁽²⁾;
- c) π^-/π^+ results by a Tokyo group⁽³⁾;
- d) electroproduction on bound protons and neutrons by a Desy group⁽⁴⁾;
- e) total hadronic photon cross section on deuterium and hydrogen by a Daresbury group⁽⁵⁾.

I'll begin by discussing the results of the experiments c), d) and e) and, then, those of the bubble chambers which, until now, can be considered the most definitive ones.

In Fig. 1 we have the preliminary results of the Tokyo group⁽³⁾. These data are consistent with the absence of an isotensor current, as can also be seen in Fig. 2.

Some attention should be paid to the fact that the π^- cross section obtained by means of the π^- to π^+ ratio may be affected by some deuteron effect, as we will see later, especially when only the pions are measured in the final state.

Fig. 3 gives the $p\pi^- \rightarrow \gamma n$ differential cross section measured by a Berkeley group⁽⁶⁾, suitably modified by means of the detailed balance principle, and the $\gamma n \rightarrow p\pi^-$ cross section as obtained by the Tokyo group. This comparison gives direct information about the T invariance properties of the electromagnetic interactions.

As we will see, all the experimental data available on the $\gamma n \rightarrow p\pi^-$ reaction are not in agreement with the Berkeley results on the inverse reaction in the first resonance region.

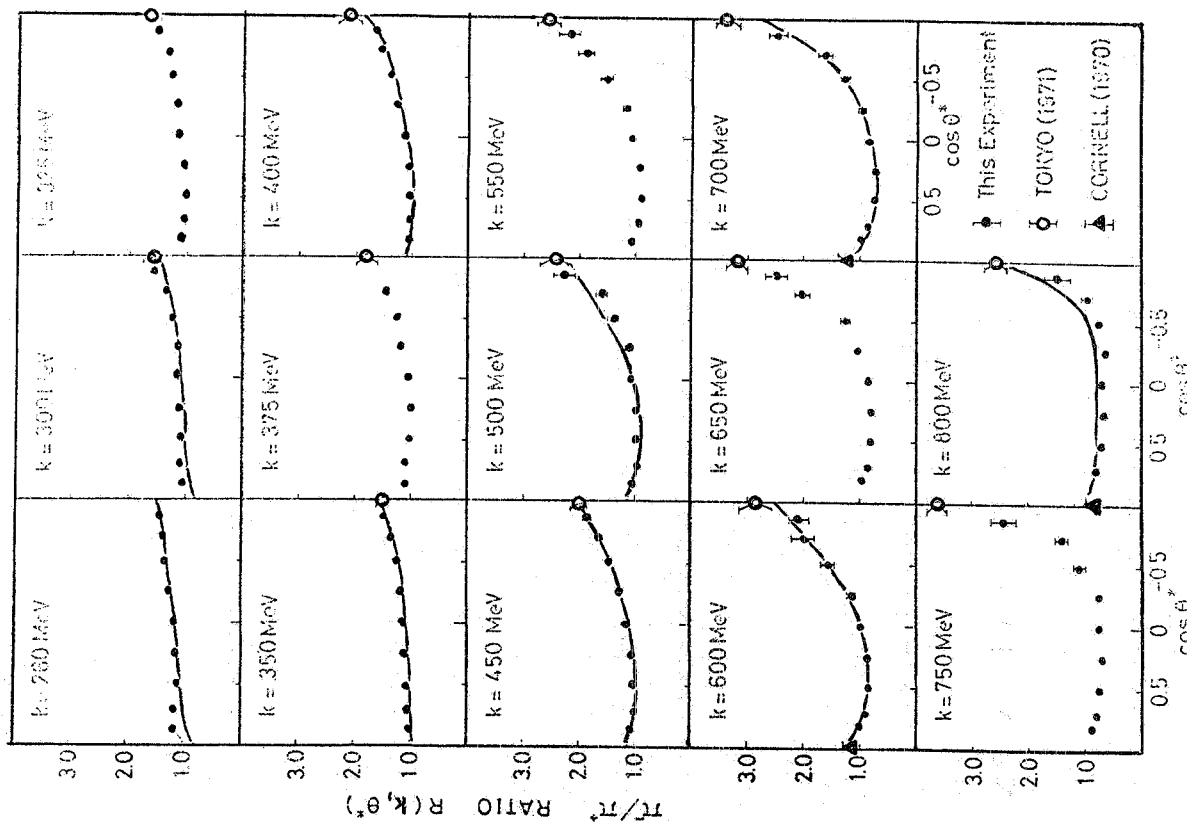


FIG. 1 - The π^-/π^+ ratio from deuterium, by Fuji et al. (3) as a function of $\cos \theta^*$ at 14 photon energies from 260 MeV to 800 MeV. The solid curves are calculated with the amplitudes of Walker's analysis.

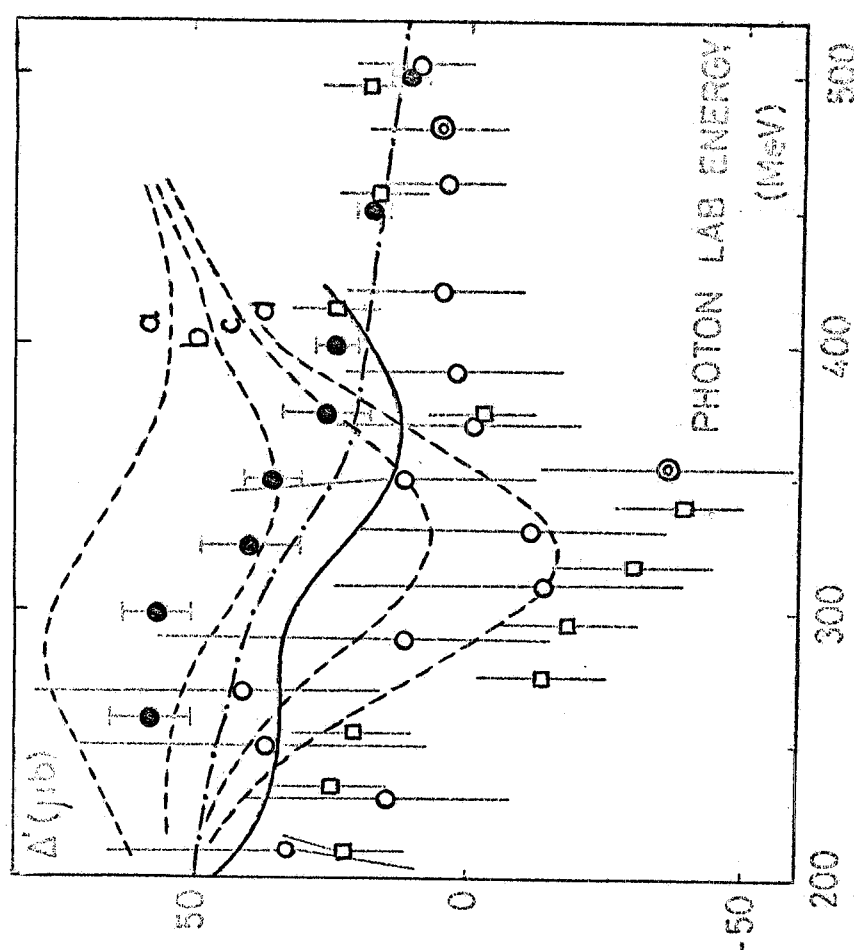


FIG. 2 - The energy dependence of $\Delta(k)$. Closed circles are obtained from the π^-/π^+ ratio data of Fuji et al. (3), open circles are from the old data of ABBHHM(1), squares are from the old data of FNP(2) and double circles are from the data of inverse reaction (16). Dotted lines show predictions by Sanda and Shaw (17) where a, b, c and d correspond to $x = 0.0, -0.1, -0.2$ and -0.3 respectively. Solid line is a prediction by Noelle and Pfeil (20), dot-dash line is by Walker (19).

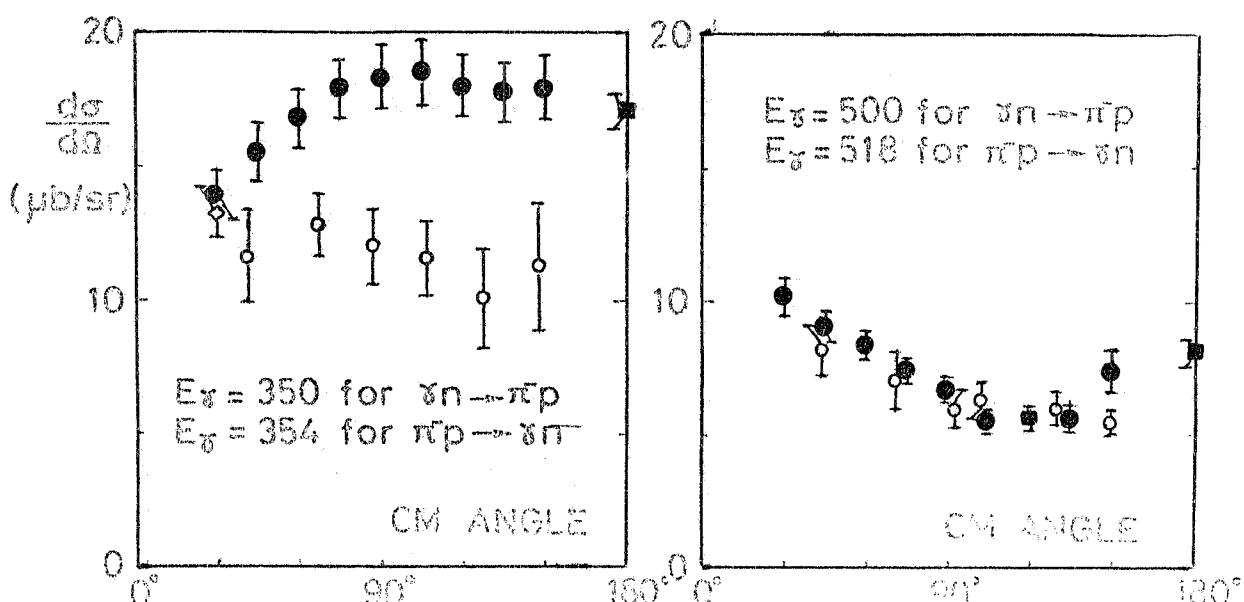


FIG. 3 - Differential cross-section for $\gamma n \rightarrow \pi^-$ at $k = 350$ MeV and 500 MeV. Closed circles are results by Fujii et al.⁽³⁾, closed square is a result of direct measurement at 180° ⁽²¹⁾, open circles and a diamond show results obtained from the inverse reaction by Berardo et al.⁽¹⁶⁾ and Favier et al.⁽²²⁾, respectively.

Another experimental result consistent with no isotensor contribution is shown in Fig. 4. In this experiment by a Desy group⁽⁴⁾ the cross section for electroproduction on protons and on neutrons is investigated and the difference of the total electroproduction cross section on bound protons and neutrons as a function of the invariant masses for different four-momentum transfers is shown.

Furthermore, they separate the cross section into a resonant cross section σ_{res} corresponding to the excitation of the $A_{33}(1236)$ isobar and the nonresonant background contribution σ_{nres} .

The difference of the resonant cross sections is plotted in Fig. 5 for the electro-excitation of the A_{33} resonance on protons and on neutrons. Any difference in the resonant cross sections would be due to the isotensor current.

The errors quoted in this measurement are rather high. As result we can consider these data as not inconsistent with the absence of an isotensor current.

Finally, some recent data from Daresbury⁽⁵⁾ on the γd total photon hadronic cross section do not seem to exclude the effect of an isotensor contribution. Fig. 6 shows the total γd cross section, corrected for the deuteron smearing effects, compared with the total γp cross section as measured on free protons.

One expects that the total cross section in deuterium is larger than twice the total cross section on protons in the absence of an isotensor contribution.

Before considering the bubble chamber experiments, let me get into some technical problems concerning the use of the deuterium as a neutron target. This is necessary in order to have a fair judgement of the reliability of the data.

We can divide the deuterium effects into two classes. Firstly there are the dynamical effects, which cannot be exactly calculated and secondly the kinematical effects due to the motion of the interacting nucleon. These latter can be calculated to a reasonable degree of accuracy.

The effects of the first kind are :

- a) the so-called Glauber⁽⁷⁾ effects, i. e. shadow and multiple scattering effects;
- b) the Coulomb interaction⁽⁸⁾ in the final state;

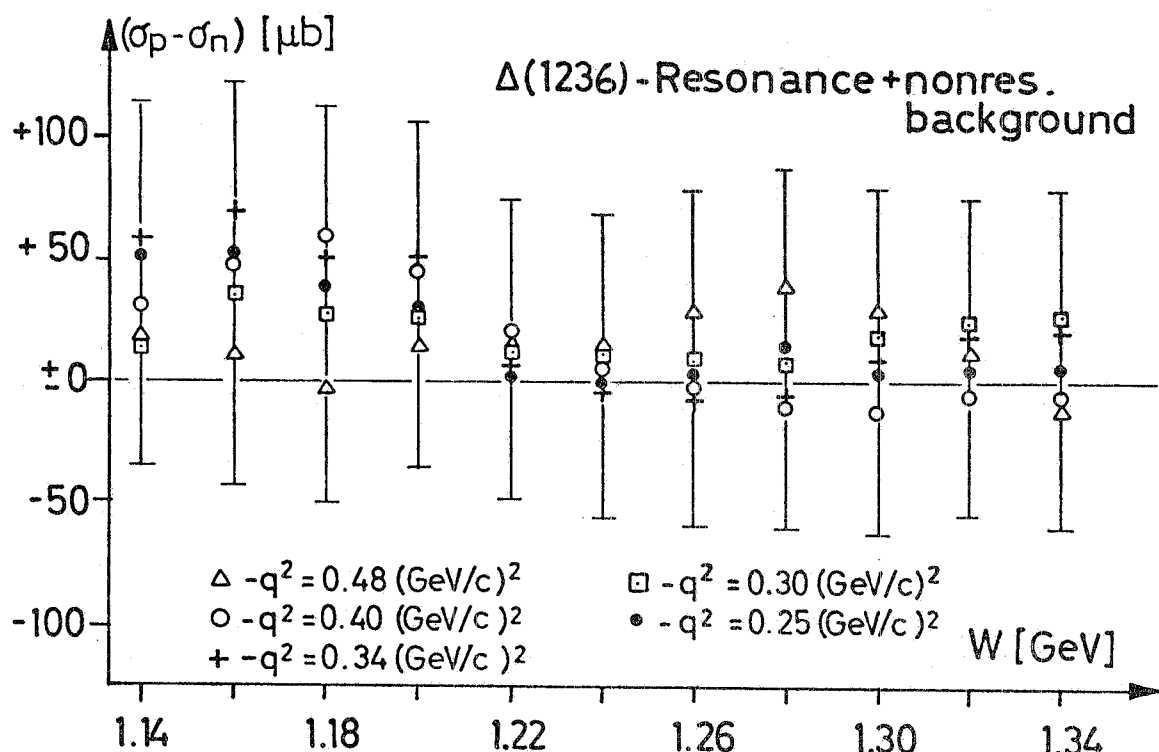


FIG. 4 - Difference of total neutron and proton electroexcitation cross section by Bleckwenn et al. (4). The errors bars include statistical and systematical errors as well as uncertainties due to radiative corrections.

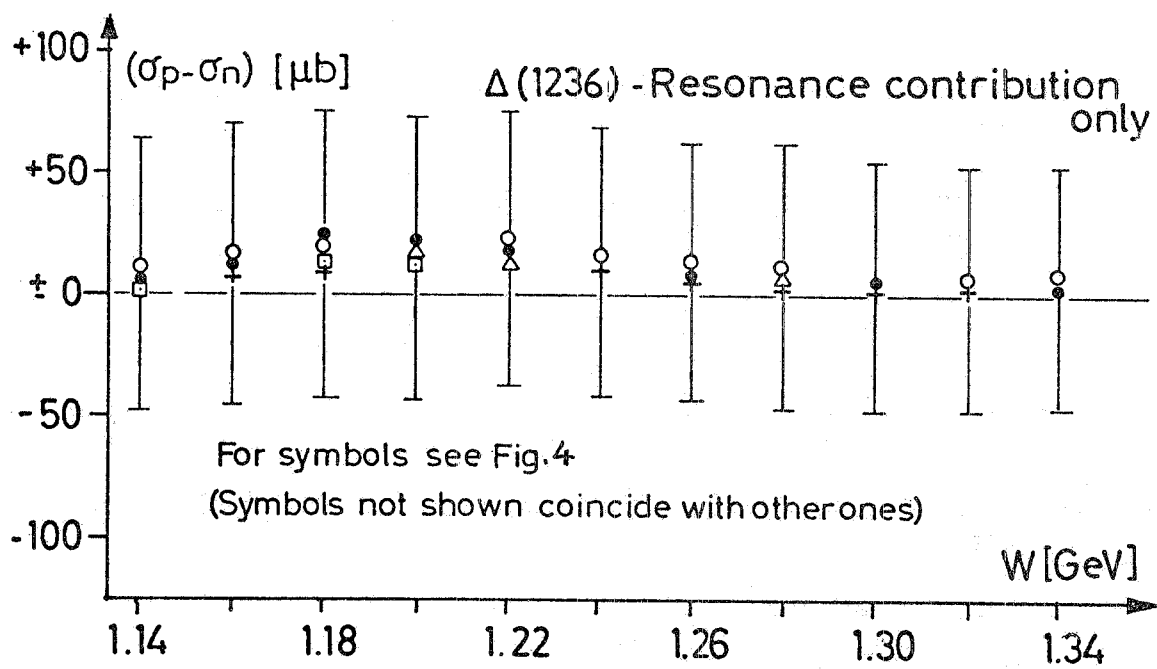


FIG. 5 - Difference of the resonance part of the neutron and proton electroexcitation cross section by Bleckwenn et al. (4).

- c) the Pauli principle, which reduces the available phase space;
- d) other kinds of final state interactions of the outgoing particles.

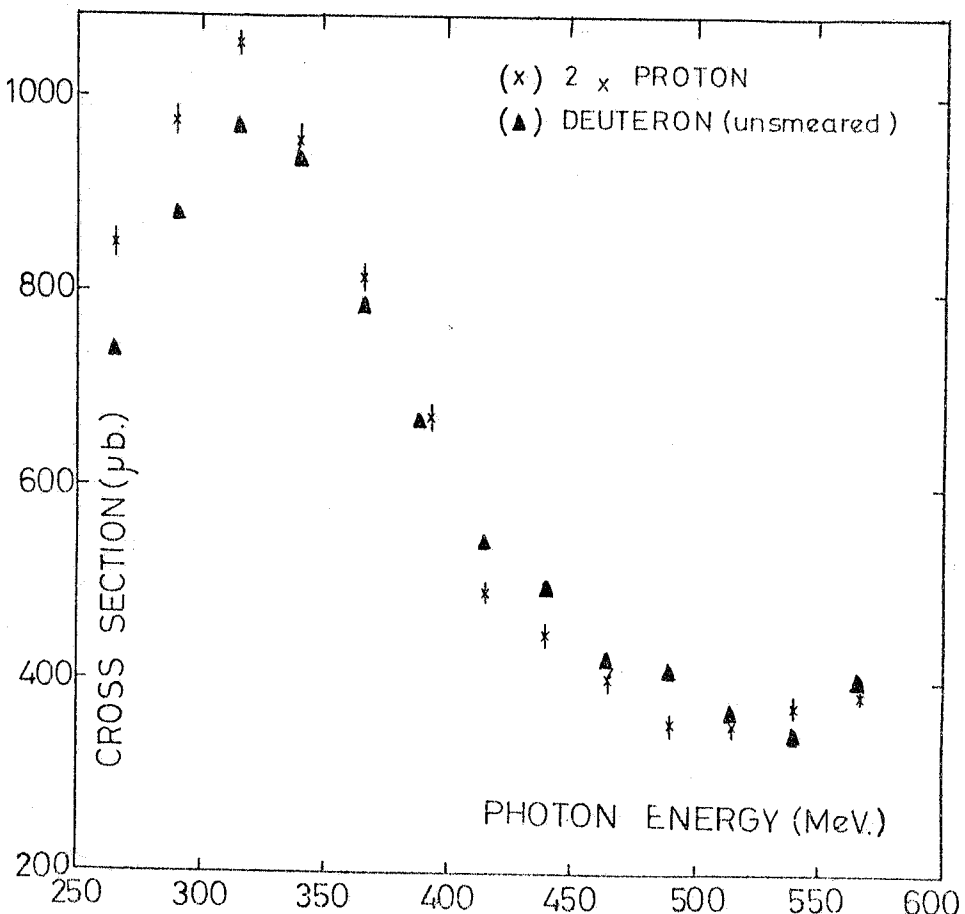


FIG. 6 - Deuteron total cross section data, by Armstrong et al. (5), corrected for internal motion of the nucleons (\blacktriangle), compared with twice that of measured $\sigma_t^P(x)$.

As it is well known, the γn cross section obtained by the measurements of the π^-/π^+ ratio in deuterium is corrected for all the above effects with the exception of Coulomb interaction. These Coulomb effects are important only near threshold, decrease rapidly with energy and are negligible in the resonance region (18).

We can only try to give an evaluation of these effects. For example, in analysing the $\gamma d \rightarrow pp\pi^-$ reaction the ABHHM collaboration (9) used the closure approximation (10). By means of this method the Pauli principle is taken into account, even if in a model dependent way. The correction found at the peak of the first resonance is of the order of 6%.

As far as the final state interaction is concerned, a recent work by Baldini and Sciacca (11) shows that the correction, due to this effect, crosses the zero at 300 MeV of γ energy and is of the same order as the mentioned Pauli correction, but goes in the opposite sense for energies lower than 300 MeV. The shadow effect (7) is expected to be less than 1%.

From this one infers that an overall correction of about 6-7% at most, due to these effects, seems to be reasonable.

Kinematical corrections take account of the fact that:

- a) the target nucleon is moving in the lab. system;
- b) the mass of the target nucleon is off mass shell and is different for each event;
- c) not all the neutron targets are kinematically accessible for a given energy of the incident γ -ray (12), i.e. it is not always possible for a low energy photon to bring nucleons, which

are in the high momenta tail of the Fermi distribution, on the mass shell.

The overall correction due to all of them is of the order of 15-20%. They are therefore the most important, but fortunately they can be calculated.

The cross sections obtained from the π^-/π^+ ratio are to be corrected also for these effects, especially for the second one.

Due to a) and b) the deuteron cross sections are smeared and shifted in energy and due to c) they are reduced with respect to the free nucleon cross sections.

The most general way to get the cross section on free nucleon using deuterium data, and taking into account all the deuterium effects, is provided by the Chew and Low⁽¹³⁾ method, which consists in extrapolating the double differential cross section $\frac{\partial^2 \sigma}{\partial E^* \partial p_s}$ to the neutron pole. This method has the disadvantage that one does not know the curve along which to extrapolate. So, only if very high statistics in the region of very small spectator momenta are available, it can be used.

If we are able to select those events which can be described by the diagram of Fig. 7⁽¹⁴⁾ (spectator model), under the reasonable assumptions that the cross section on the off mass shell nucleon is the same as on a free nucleon and that the total cross section only depends on the c. m. energy of the (γn^*) system, we can determine the photoproduction cross section on neutrons.

The model provides the expected kinematical distributions of the spectator nucleon to be compared with the experimental ones.

In Fig. 8 we have the experimental and the expected distributions⁽²⁾ of the spectator momenta. As one can see, the agreement is good for momenta lower than 250-300 MeV/c.

In this figure the effect of the "kinematic inaccessibility"⁽¹²⁾ is evident. The highest spectator momenta are forbidden for the low energy γ -rays. So, the good overall agreement in the low γ energy region between the model and the experimental results is only in the appearance and these distributions are not very effective in selecting those events that better agree with the spectator model.

The FNPR collaboration⁽¹⁵⁾ uses a more selective criterion, based on the angular distributions of the spectator in the γd c. m. s. These distributions are shown in Fig. 9 for various E_γ intervals.

Since this distribution is expected to be somewhat broadened in a three body interaction, it seems reasonable to introduce a cut in this angle, which, on the other hand, is expected to have a very narrow distribution in the spectator model.

In Fig. 10 the momentum distributions of the spectator proton are shown for values of $\cos \theta_s^*$ higher and lower than the cut value. The effect of the cut is evident and the agreement between experiment and prediction is now very satisfactory.

One can therefore conclude that the predictions of the spectator model are well verified by the deuterium data, after having applied the above cut.

The Desy group uses three methods for getting the γ -n cross section starting from the deuterium data.

The results obtained with the spectator model, selecting those events in which the spectator momentum is lower than 300 MeV/c, are shown⁽¹⁶⁾ in Fig. 11.

Fig. 12 shows the cross section⁽⁹⁾ obtained without any event selection and without spectator identification, using the closure approximation⁽¹⁰⁾. This cross section is also corrected

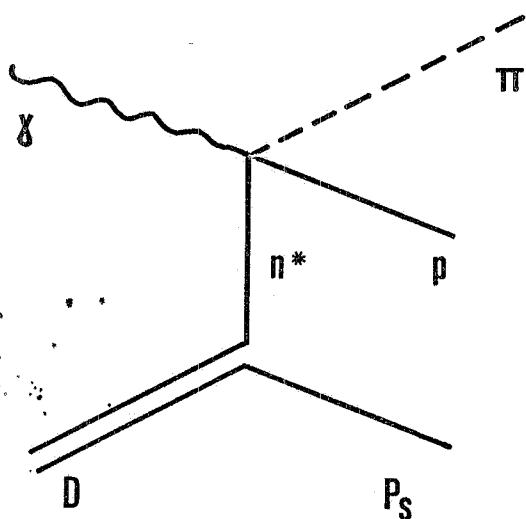


FIG. 7 - Diagram assumed to describe the reaction $\gamma d \rightarrow p \pi^-$, p_s , according to the spectator model.

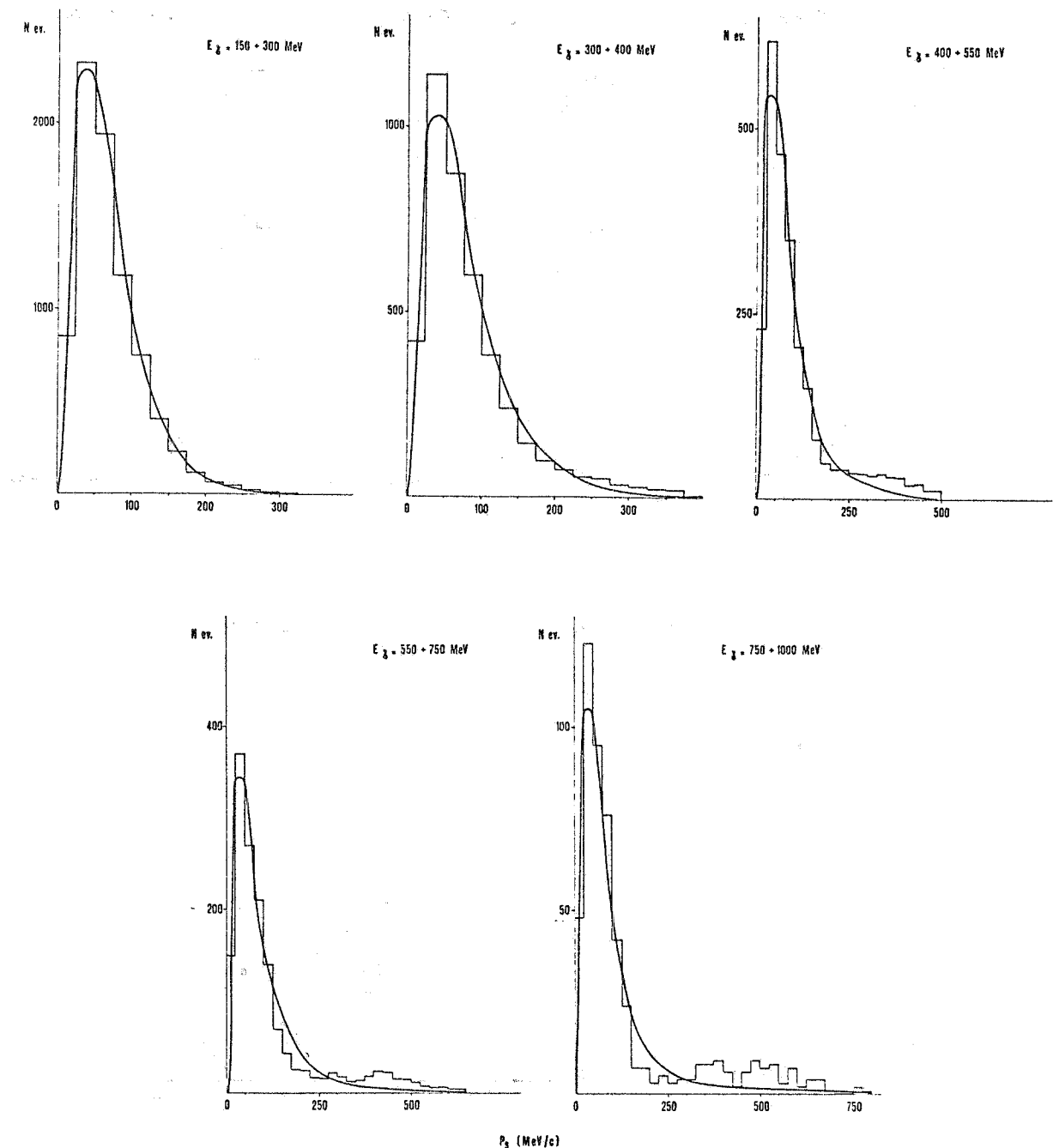


FIG. 8 - Momentum distribution⁽¹⁵⁾ of the spectator proton for various intervals of the photon energy (in the L. S.). The curves show the predictions of the spectator model, including the kinematical effects.

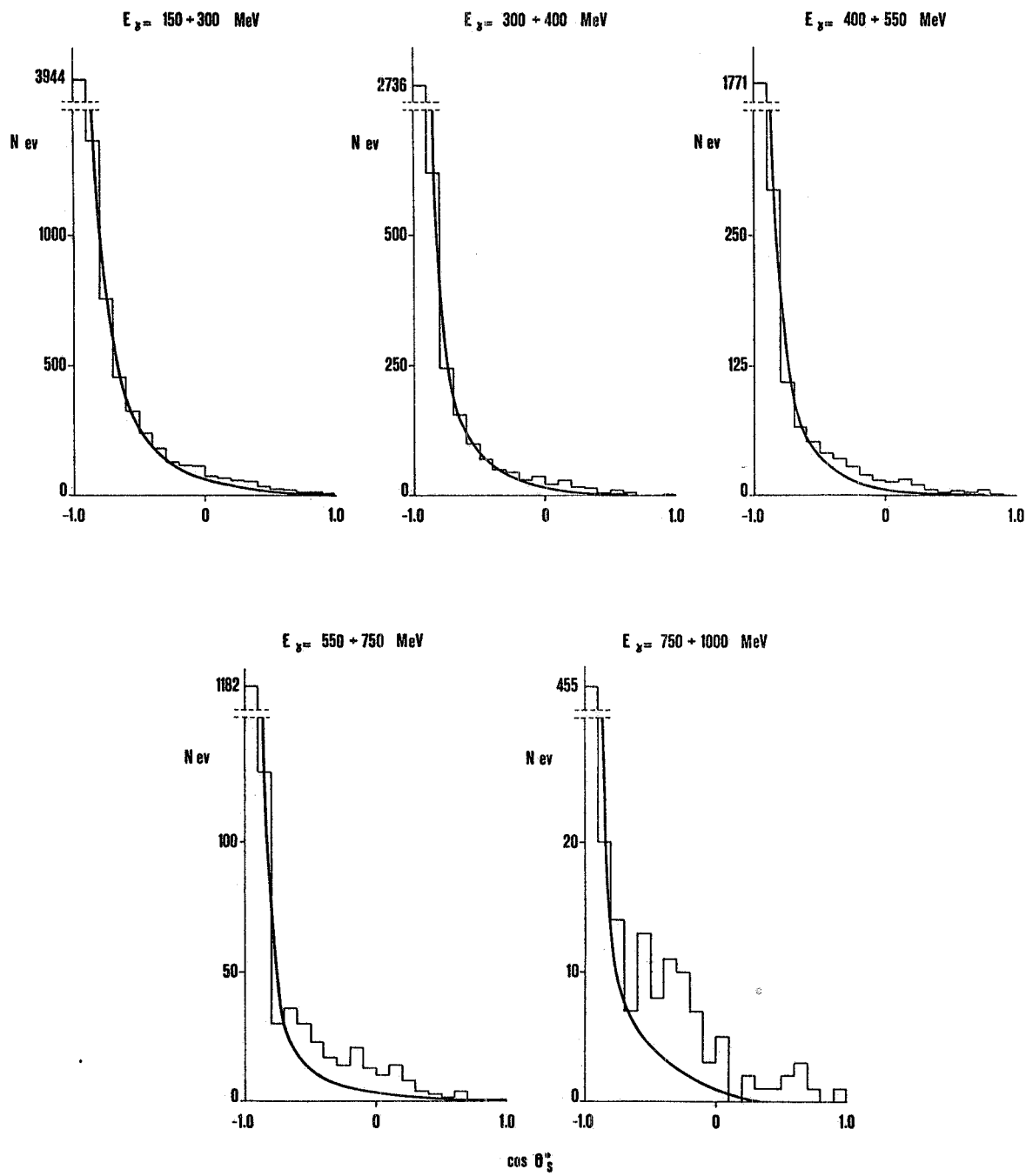


FIG. 9 - Angular distribution⁽¹⁵⁾ of the spectator proton in the γd c.m.s.
The curves show the predictions of the spectator model.

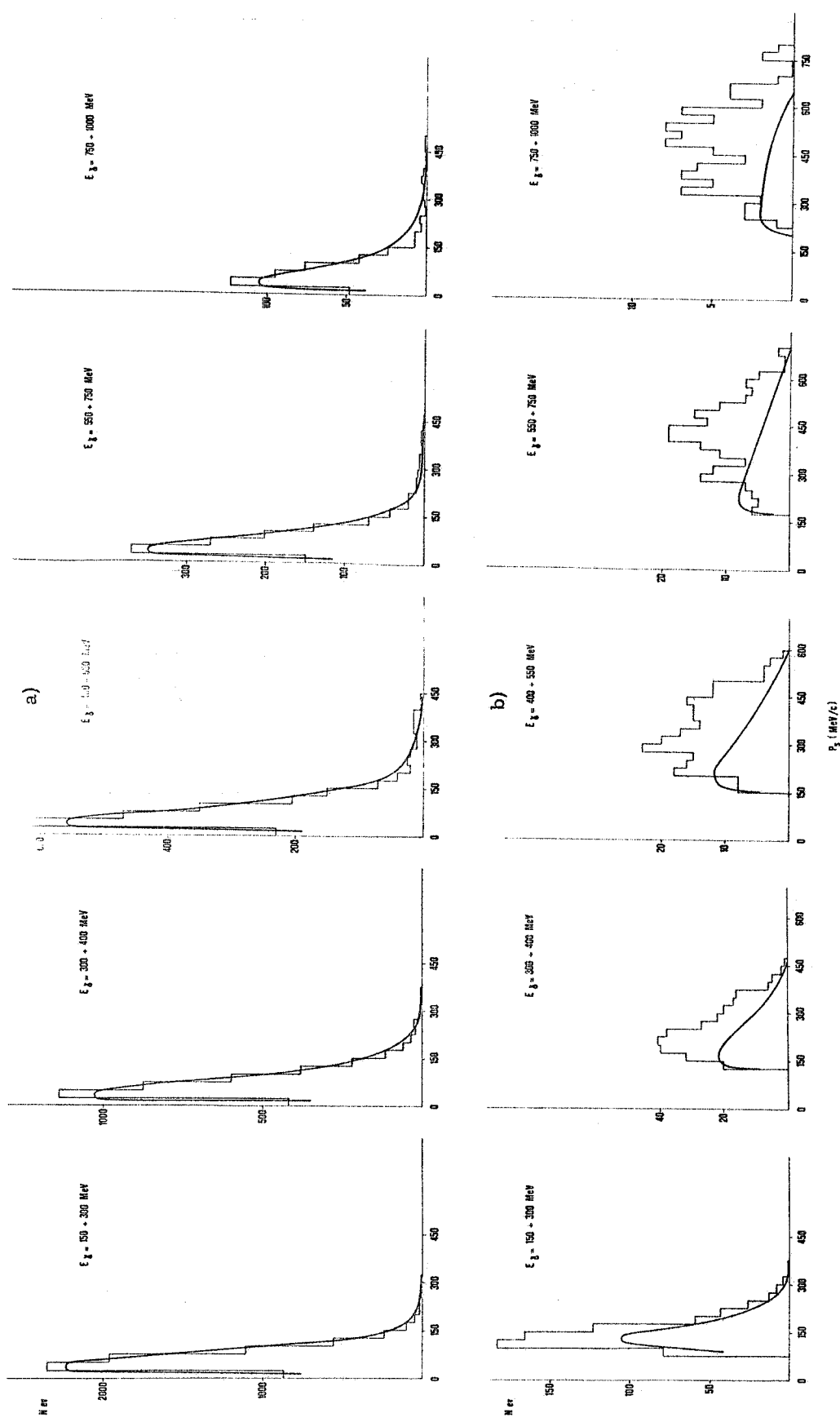


FIG. 10 - Same of Fig. 8, but after the θ_s^* cut(15): a) for $\cos \theta_s^* < \cos \theta_{os}^*$; b) for $\cos \theta_s^* > \cos \theta_{os}^*$. The curves, representing the predictions of the spectator model, are normalized to the events with $\cos \theta_s^* < \cos \theta_{os}^*$.

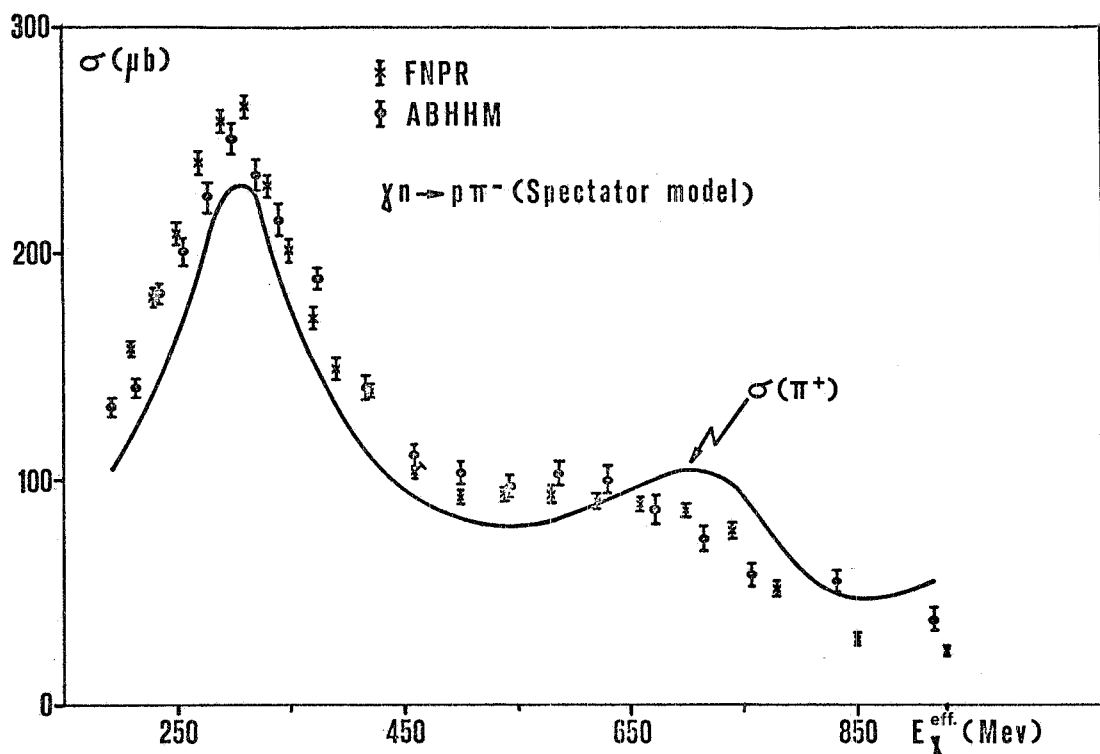


FIG. 11 - Total cross section of the reaction $\gamma n \rightarrow p\pi^-$, from the ABHHM collaboration⁽¹⁶⁾, as obtained using the spectator model (x). For comparison are also reported the results from FNPR collaboration⁽¹⁵⁾ (□). The superimposed curve is the cross section for $\gamma p \rightarrow p\pi^+$.

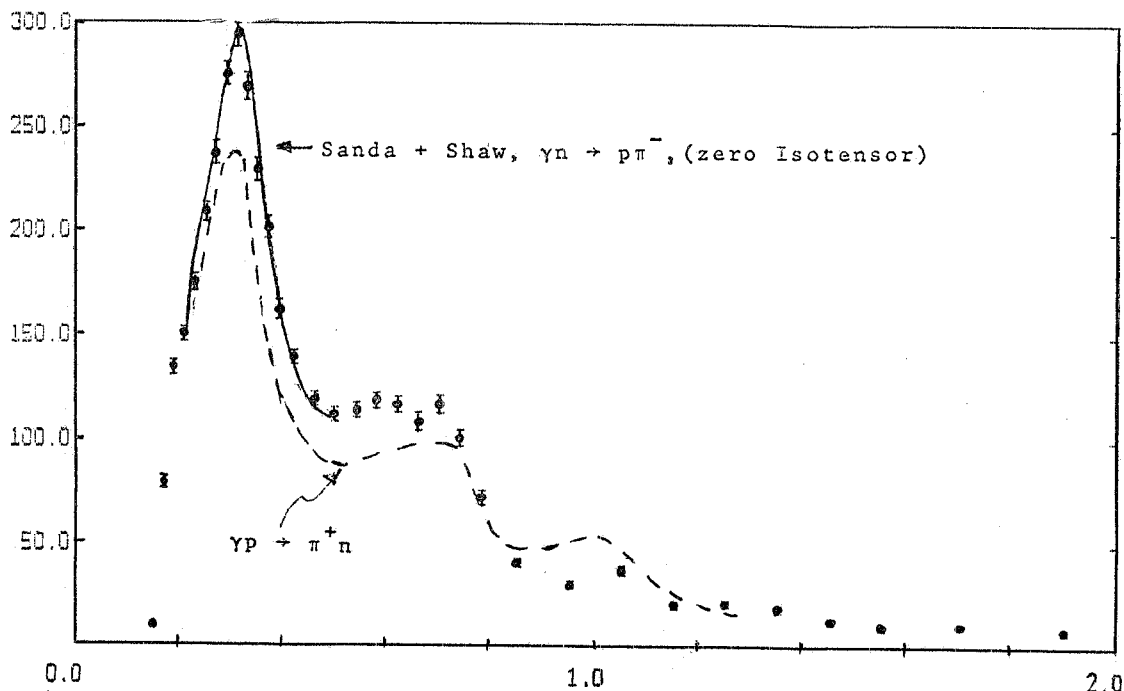


FIG. 12 - Total cross section of the reaction $\gamma n \rightarrow p\pi^-$ from ABHHM collaboration⁽⁹⁾, as obtained using closure approximation⁽¹⁰⁾. The full curve shows the prediction of ref. (17) with zero isotensor contribution; the dashed curve shows the behaviour of $\sigma(\gamma p \rightarrow n\pi^+)$.

for the effect of Pauli principle.

It should be noted that this method can be applied only if the spin-flip and non-spin-flip photoproduction amplitudes on neutron are known, so the Pauli corrections depend on the model used in evaluating these amplitudes.

The ABHHM collaboration⁽¹⁶⁾ also tried to use the Chew-Low method. In Fig. 13 the extrapolation for E_γ in the interval 280-300 MeV is reported. The total cross section obtained with this method is shown in Fig. 14.

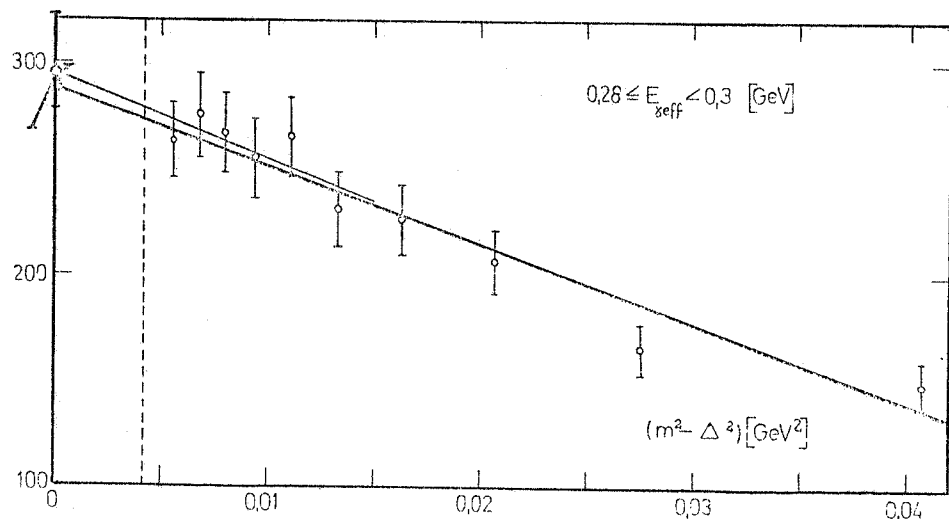


FIG. 13 - Chew-Low extrapolation function (μb) as a function of $(t - m_n^2)^2$ (GeV^2). The lines show linear fits to the data in two different ranges of t . At the left the extrapolated value of the cross section at the n pole can be seen⁽¹⁶⁾.

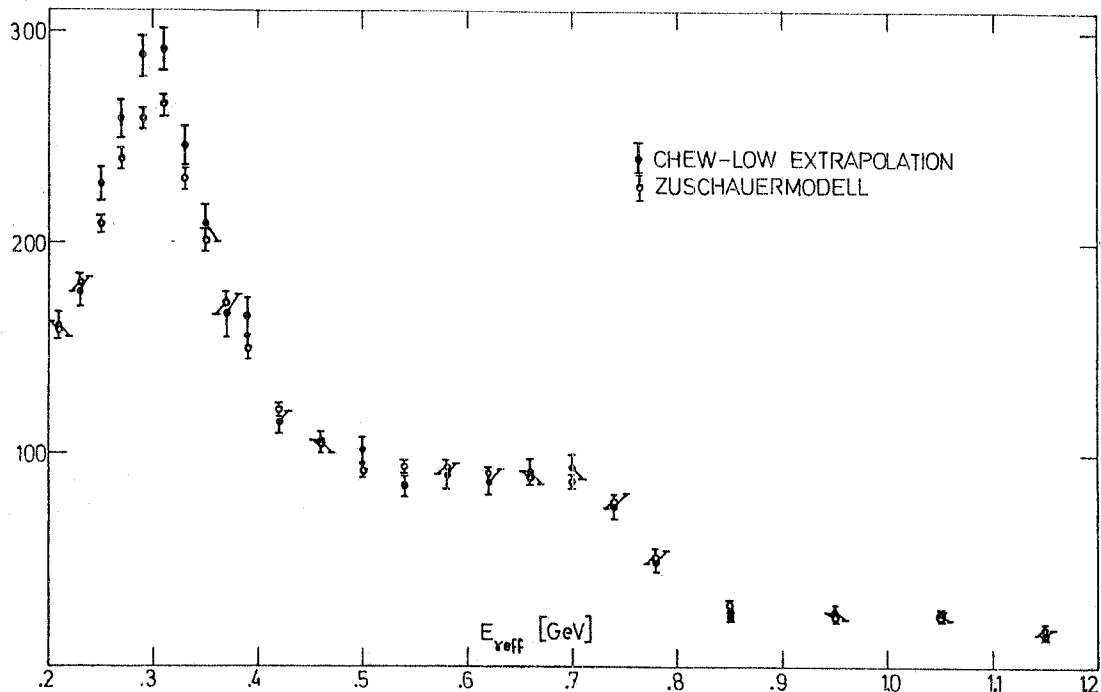


FIG. 14 - The total cross section of reaction $\gamma n \rightarrow p\pi^-$ as obtained by Chew-Low extrapolation from the ABHHM collaboration⁽¹⁶⁾ (●). The results of the spectator model are also reported for comparison (○).

The results of the closure approximation and of the Chew-Low extrapolation are in good agreement in the first resonance region and give a cross section higher than that given by the spectator model. For higher energies the agreement between the Chew and Low method and the spectator model becomes satisfactory and the cross sections so obtained are smaller than those given by the closure approximation.

Figs. 15 and 16 show the difference Δ of the Sanda and Shaw test⁽¹⁷⁾ obtained using the results of the closure approximation and the comparison with the results of the inverse reaction. As one can see, the data agree with no isotensor contribution.

As concerns the problem of T-reversal invariance, there is strong disagreement between the $\gamma n \rightarrow p\pi^-$ differential cross section and that of the inverse reaction in the region of the first resonance, while for higher energies the agreement is fairly good.

As we have seen the FNPR group makes use of the spectator model, but in a more sophisticated way, by selecting the events according to the spectator angle in the γd center of mass system.

The total cross section as measured⁽¹⁵⁾ by this group is shown in Fig. 17 and the result of the isotensor test is shown in Fig. 18.

In this case an isotensor contribution cannot be excluded.

In Fig. 19 again the $p\pi^- \rightarrow \gamma n$ differential cross section⁽⁶⁾, modified by means of the detailed balance principle, is reported, as well as the $\gamma n \rightarrow p\pi^-$ cross section as obtained by a Moravcsik⁽¹⁸⁾ fit to the FNPR data. The shaded band contains two standard deviations about the calculated values.

As one can see, also in these results there is strong disagreement only in the first resonance region.

Now let me critically compare the ABHHM and FNPR results.

If we consider the FNPR⁽¹⁷⁾ results corrected for the Pauli exclusion principle with the same coefficients, as the ABHHM one, we find a difference of 9% with respect to the ABHHM results in the first resonance peak.

Now, if we compare the unprocessed $\gamma d \rightarrow pp\pi^-$ cross sections (Fig. 20) we find a disagreement of the same order.

So, the main difference between the results of these two experiments comes out from the unprocessed data and not from the procedure used for getting neutron cross section.

What conclusions can one draw from the present experimental situation?

As far as the violation of time reversal invariance is concerned we have seen that all the experiments give a $\gamma n \rightarrow p\pi^-$ cross section higher than the one derived from the data of the Berkeley group⁽⁶⁾ on the inverse reaction.

On the other hand, we must consider that the measurement of the $\pi^- p \rightarrow \gamma n$ reaction is not so easy and only one experiment on this reaction is certainly not sufficient to allow definitive conclusions on this problem.

The situation concerning a possible isotensor contribution to the e.m. current seems until now unsolved, different experiments giving different results.

The first point to define is what is the true value of the $\gamma d \rightarrow pp\pi^-$ cross section; the second one is to ascertain real importance of the Pauli exclusion principle and the final state interaction effects.

I think that the measurements of the π^-/π^+ ratio are very important in this respect, but it is necessary to take into account all the deuteron kinematical effects.

Furthermore, an experimental investigation on the π^0 photoproduction on neutrons would be useful. Indeed this reaction is very sensitive to the isotensor contribution and the knowledge of the four single pion photoproduction channels would allow a determination of this contribution in a completely model independent way.

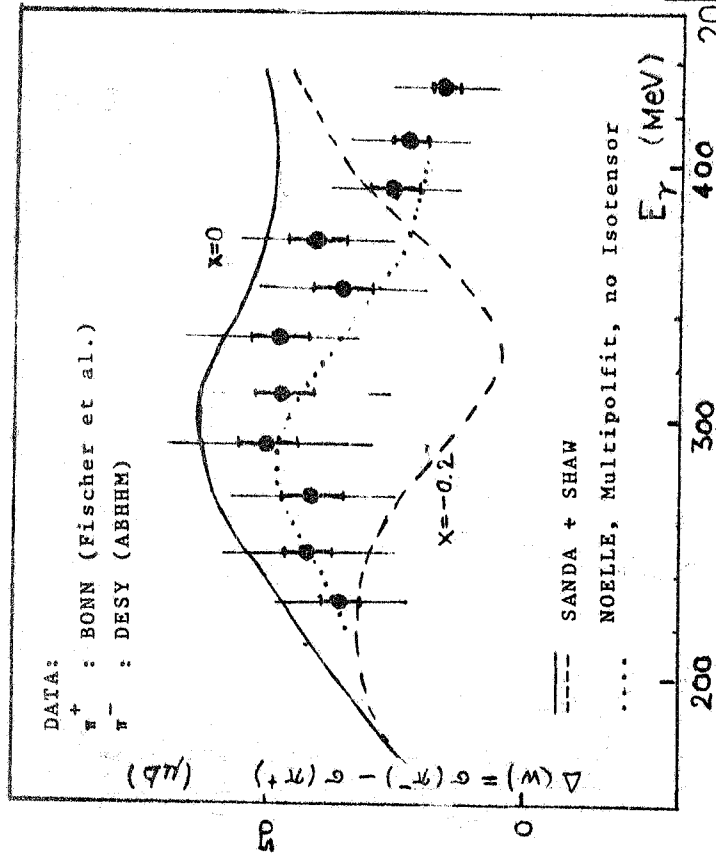


FIG. 15 - The energy dependence of $d\sigma/d\Omega$ from the ABHHM collaboration(9). The previsions of Sanda and Shaw⁽¹⁷⁾ are also reported ($x = 0.0$ full line; $x = -0.2$ dashed line). Dotted line is a prediction by Noelle and Pfeil⁽²⁰⁾ for no isotensor contribution.

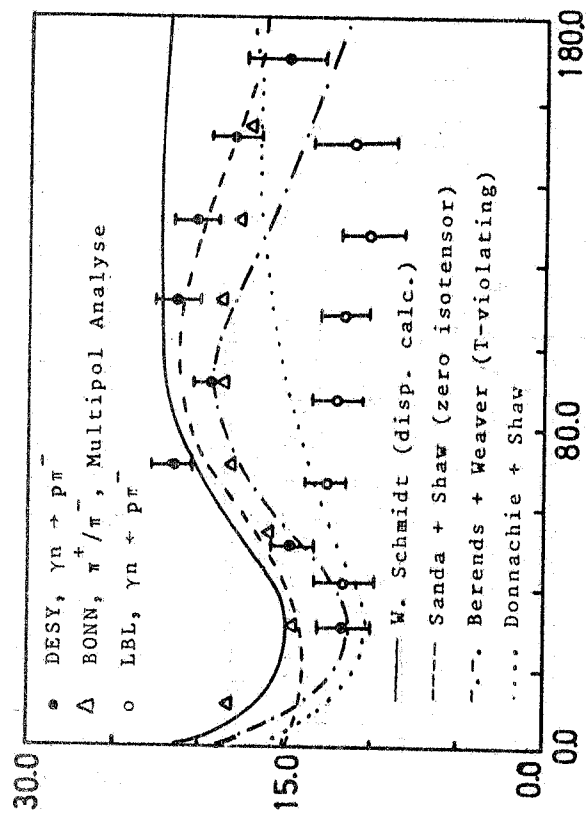


FIG. 16 - CMS differential cross section $d\sigma/d\Omega$ of the reaction $\pi^- p \rightarrow \pi^- n$ from the ABHHM collaboration. Curves show predictions by Engels et al. (22) (full), Sanda and Shaw⁽¹⁷⁾ (zero Isotensor) (dashed), Behrends and Weaver⁽²³⁾ (dash-dotted). Also shown are results (ϕ) by Berardo et al.⁽⁶⁾, predicted from the inverse reaction $\pi^- p \rightarrow \pi^- n$.

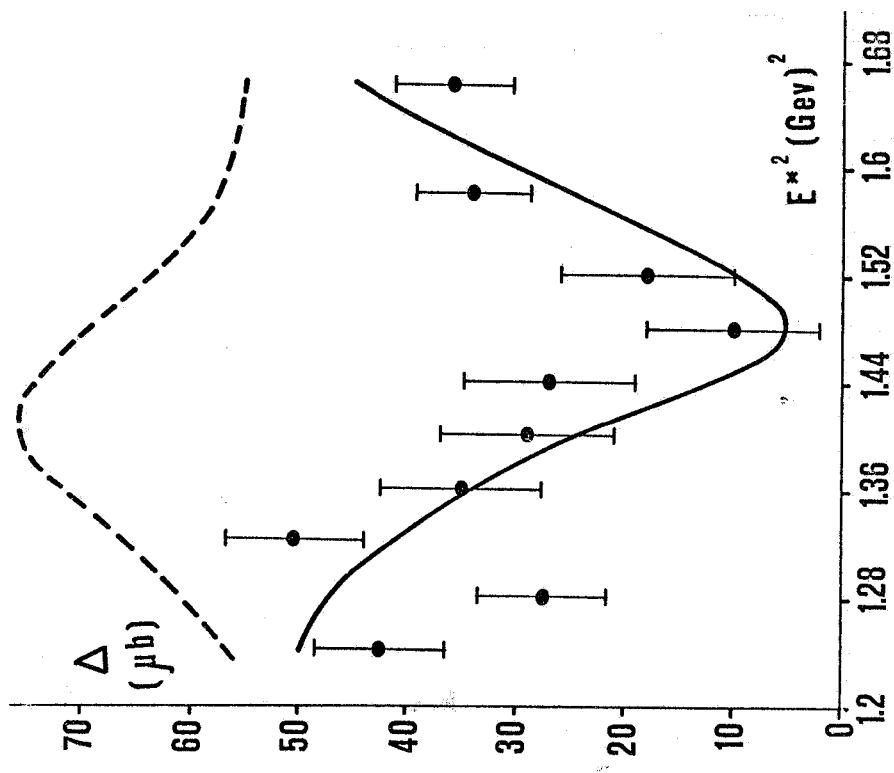


FIG. 18 - The energy dependence of $\Delta(k)$ from the FNPR collaboration(15). The curves are the predictions of Sanda and Shaw(17) with $x = -0.2$ (full line) and $x = 0.0$ (dashed line).

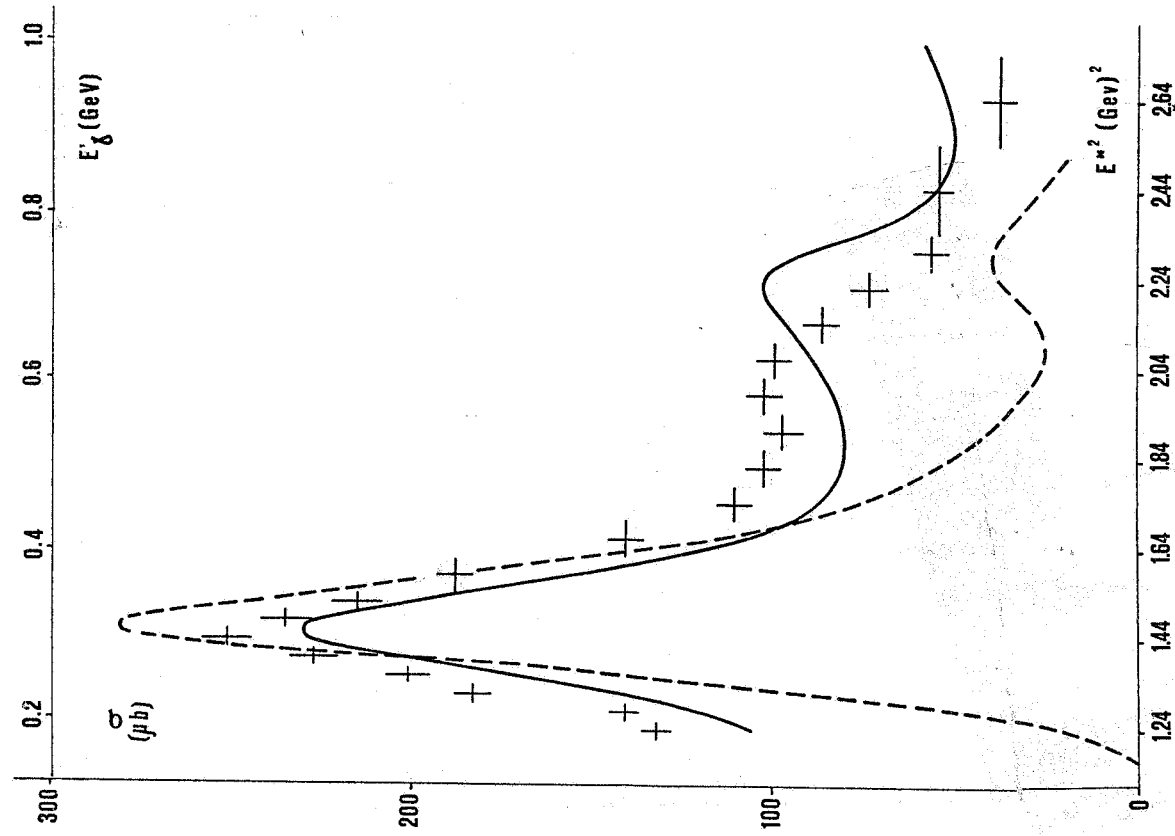


FIG. 17 - Total cross section for the reaction $\gamma n \rightarrow p\pi^-$ from the FNPR collaboration(15). The curves are the cross sections for $\gamma p \rightarrow p\pi^0$ (dashed line) and $\gamma p \rightarrow p\pi^+$ (full line).

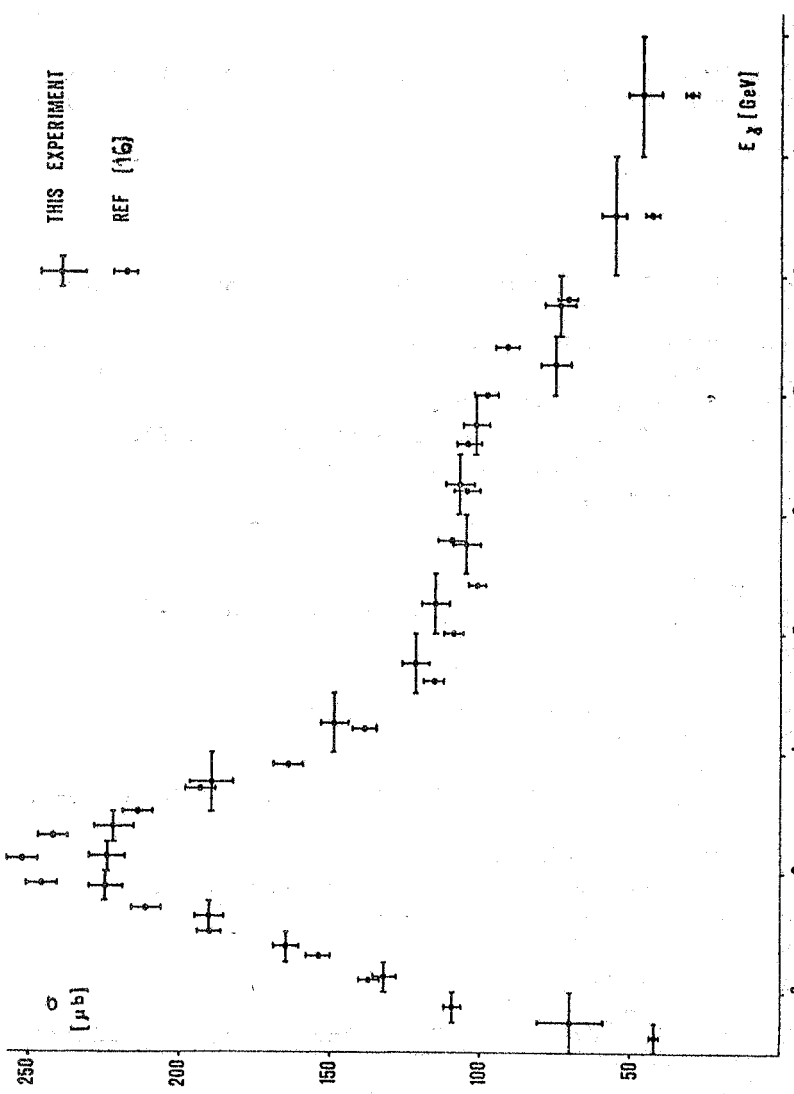
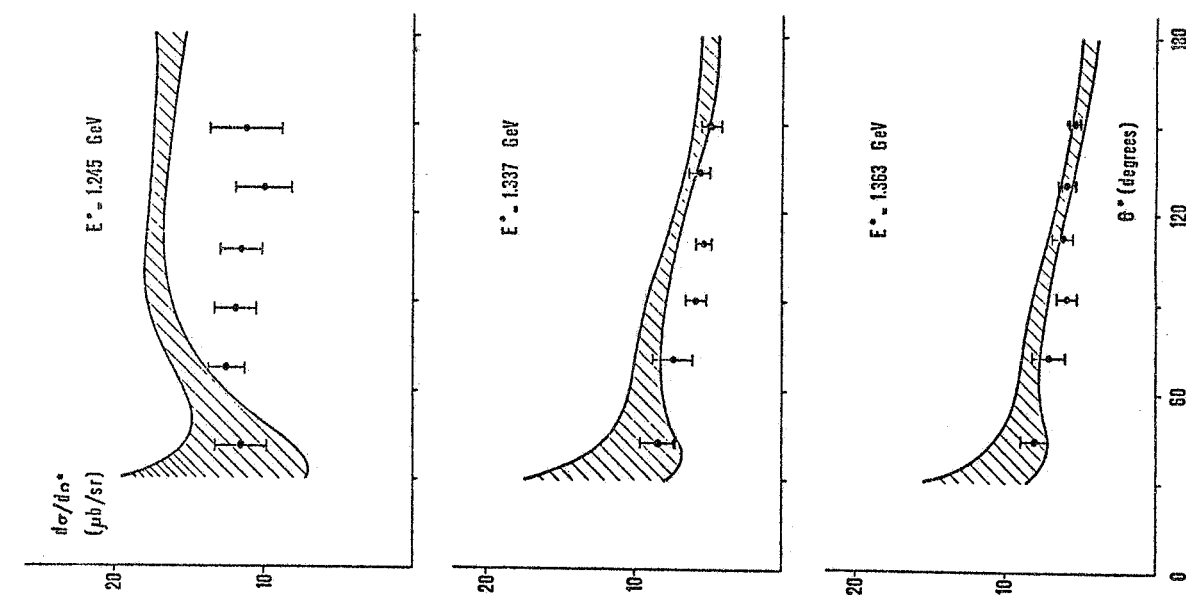


FIG. 20 - Comparison between the $\gamma d \rightarrow pp\bar{\pi}$ cross sections as measured by the ABHHM collaboration(16) (\bullet) and by the FNPR collaboration(15) (\square).

FIG. 19 - CMS differential cross sections $d\sigma/d\Omega$ of the reaction $\gamma n \rightarrow p\pi^-$ as obtained by a Moravcsik fit on the FNPR collaboration data(15). The shaded band contains two standard deviations about the calculated values. Results by Berardo et al. (6) for $\pi^-p \rightarrow n\bar{y}$ are shown for comparison.

Acknowledgements. -

I wish to thank the ABHHM collaboration and in particular drs. P. Benz, H. Kowalski, K. Müller and P. Söding for the interesting discussions held during the preparation of this talk.

REFERENCES. -

- (1) - Aachen-Berlin-Bonn-Hamburg-Heidelberg-Munich (ABBHHM) Collaboration, Nuclear Phys. B8, 535 (1968).
- (2) - Frascati-Napoli-Pavia-Roma (FNPR) Collaboration, Lett. Nuovo Cimento 3, 697 (1970); Lett. Nuovo Cimento 2, 1183 (1971).
- (3) - T. Fujii et al., Tokyo University Report INS-184 (1972).
- (4) - J. Bleckwenn et al., Desy Report 71/63 (1971); Phys. Letters 38B, 265 (1972).
- (5) - T. A. Armstrong et al., Daresbury Report DNPL/P-105 (1972).
- (6) - P. A. Berardo et al., Phys. Rev. Letters 26, 201 (1971).
- (7) - R. J. Glauber, Phys. Rev. 100, 242 (1955); V. Franco and R. J. Glauber, Phys. Rev. 142, 1195 (1966).
- (8) - A. Baldin, Nuovo Cimento 8, 569 (1958).
- (9) - P. Benz et al. (ABHHM Collaboration), Intern. Symp. on Electron and Photon Interactions at High Energies, Cornell (1971).
- (10) - G. F. Chew and H. W. Lewis, Phys. Rev. 84, 779 (1951).
- (11) - R. Baldini-Celio and G. Sciacca, Frascati Report LNF-71/92 (1971).
- (12) - D. M. White et al., Phys. Rev. 120, 614 (1960).
- (13) - G. F. Chew and F. E. Low, Phys. Rev. 113, 1640 (1959).
- (14) - G. F. Chew and G. Wick, Phys. Rev. 85, 636 (1952); G. F. Chew and M. L. Goldberger, Phys. Rev. 87, 778 (1952).
- (15) - FNPR Collaboration, Frascati Report LNF-72/31 (1972).
- (16) - K. Müller (ABHHM Collaboration), Bonn University Report PIB 3-20 (1971).
- (17) - A. I. Sanda and G. Shaw, Phys. Rev. Letters 24, 1310 (1970).
- (18) - M. I. Moravcsik, Phys. Rev. 104, 1451 (1956).
- (19) - R. L. Walker, Phys. Rev. 182, 1729 (1969).
- (20) - P. Noell and W. Pfeil, Nuclear Phys. B31, 1 (1971).
- (21) - T. Fujii et al., Phys. Rev. Letters 26, 1672 (1971); Phys. Rev. Letters 27, 223 (1971).
- (22) - J. Engels et al., Phys. Rev. 175, 1951 (1968).
- (23) - F. A. Behrends and D. L. Weaver, Phys. Rev. 4D, 1997 (1971).